: *Q. J. R. Meteorol. Soc.* (2001), **127**, pp. 1615–1626

The impact of new water vapour spectral line parameters on the calculation of atmospheric absorption

By WENYI ZHONG[1]*, JOANNA D HAIGH[1], DJEDJIGA BELMILOUD[2], ROLAND SCHERMAUL[1] and JONATHAN TENNYSON[2]
[1]*Imperial College of Science, Technology and Medicine, UK*
[2]*University College London, UK*

(Received 15 September 2000; revised 12 February 2001)

SUMMARY

New laboratory measurements and theoretical calculations of integrated line intensities for water vapour bands in the near-infrared and visible regions (8600–15 000 cm^{-1}) show a systematic 6–26% increase in band intensities compared to the HITRAN96 database. We have used the GENLN2 line-by-line code to assess the effects of such changes in the water vapour spectral database on calculations of clear-sky short-wave fluxes and heating rates. Three standard atmospheres were used and it was found that, compared with HITRAN96 results, the absorbed downward solar fluxes increase (including the effects of theoretically predicted weak water lines in the region) by 5.5, 4.8 and 2.2 W m^{-2} (solar zenith angle = 30°) and by 2.4, 2.1 and 1.1 W m^{-2} (solar zenith angle = 75°) respectively. The maximum change in heating rate is about 4%. The effects are about five to eight times larger than those produced by using the Giver *et al.* corrections. The combined effects of the revised description of the spectroscopy of water vapour account for approximately 30–90% of the absorption currently ascribed to the water vapour continuum in this spectral region.

KEYWORDS: HITRAN database Solar radiation Water vapour

1. INTRODUCTION

Calculations of solar radiative fluxes and heating rates in the visible and near-infrared regions rely on spectroscopic databases such as HITRAN96 (the HIgh-resolution TRANsmission molecular absorption database 1996 edition (Rothman *et al.* 1998): subsequently referred to as HT96). These provide spectral line positions, intensities, widths, and their temperature dependences, for gases of importance in atmospheric radiative transfer. The HITRAN database has had three major editions since the middle 1980s (Rothman *et al.* 1987, 1992, 1998). The total number of spectral lines has increased substantially with each revision, and the accuracy of the spectral parameters has also increased because of improvements in theoretical and experimental spectroscopy. However, for water vapour there has been little change since 1992 except for the introduction of more lines in the thermal infrared region. Recently the debate concerning the underestimate by model calculations of atmospheric absorption of solar radiation (e.g. Cess *et al.* 1995; Arking 1996) has turned attention on minor absorption bands and minor species (e.g. Chou 1999). However, two recent papers (Lubin *et al.* 2000; Mlawer *et al.* 2000) compared the results from spectrally detailed solar irradiance measurements with calculations based on the recent corrections to HT96 by Giver *et al.* (2000), and suggested that any unknown clear-sky absorption is of limited significance. In laboratory measurements to determine air-broadening coefficients for the water absorption lines in the visible and near-infrared regions (8600–15 000 cm^{-1}), Schermaul *et al.* (2001a,b) found that there was a systematic underestimate in HITRAN strong line intensities (by 6–26% for the sum of all line intensities of a given water polyad) and that the recent corrections to HT96 by Giver *et al.* (2000) do not remove these discrepancies, but in fact increase them to 6–38%. Moreover, the effect of thousands of weak water lines not

* Corresponding author: Department of Physics, Imperial College of Science, Technology and Medicine, London, SW7 2BW, UK. e-mail: w.zhong@ic.ac.uk

included in HT96 on the atmospheric absorption of solar radiation is also not negligible (Learner *et al.* 1999; Clerbaux 1999).

The aim of this work is to investigate the effect of the spectral line parameters derived from new laboratory measurements on radiative fluxes and heating rates in the atmosphere in the 8600–15 000 cm^{-1} spectral region. The effect of weak water lines predicted by *ab initio* theory on the vertical structure of atmospheric absorption is also estimated for a wider spectral region (1000–22 700 cm^{-1}), where direct line-by-line calculation can now replace the statistical argument of Learner *et al.* (1999).

2. Absorption line parameters used in this study

HT96 and its corrected version in the 8036–22 700 cm^{-1} regions (henceforth named COR) have been used as the control datasets to be compared with the results of experiments using two different modified versions. The first modification (called WEAK) adds theoretically calculated weak water lines to HT96; the second (ESA-WVR) includes the newly measured strong lines as well as theoretical weak lines (calculated as in WEAK) but in the 8600–15 000 cm^{-1} region. In what follows we briefly describe the new databases.

(*a*) *Theoretically calculated weak water lines*

Theoretical calculations, based on the *ab initio* potential-energy surface method (Partridge and Schwenke 1997, henceforth PS), are able to produce complete water spectra with considerable precision over a wide range of wavelengths and intensities. Using *ab initio* procedures with energy levels adjusted to spectroscopic data, the wave numbers of the synthesised linelist are close to the observed ones. Although theoretical calculations may be less accurate than the observations, they predict thousands of weak lines which cannot at present be detected in the laboratory.

Figure 1 presents examples of theoretical line distribution (solid lines) and HT96 data (dots) against line intensity in $\log_{10}(N) - \log_{10}(I)$ space, where: N is the number of lines in k, $k+1$; $I = I_0 2^k$ is the line intensity (cm^{-1}/(molecule cm^{-2})); k is the index of octave ranges; and I_0 is an arbitrary minimum intensity. In the WEAK dataset the number of lines is taken into account in the following way: near the strong end (e.g. $k \geqslant 7$ in Fig. 1(a) to (d), or $k \geqslant 4$ in Fig. 1(e) and (f)) the HITRAN line data are used; near the weak end ($k \leqslant 0$) the theoretical data are employed; in the middle regions ($0 < k < 7$ in Fig. 1(a) to (d), or $0 < k < 4$ for Fig. 1(e) and (f)) both the HITRAN data and the weak lines predicted by theory are included, the latter being defined as those theoretical lines remaining when the correct number of HITRAN lines with highest intensities are taken away. The database contains nearly 215 000 theoretical weak water vapour lines in the spectral region 900–22 700 cm^{-1}. The cut-off in line intensity is taken as 1×10^{-30} cm^{-1}/(molecule cm^{-2}). It should be noted that the intensity decreases more rapidly than the number of lines increases: the sum over all lines converge to a well-defined limit, and the cut-off chosen includes more than 99.9% of the total absorbtance.

(*b*) *New measurements for water vapour in the 8600–15 000 cm^{-1} spectral region*

Using high-resolution Fourier transform spectrometry and multiple-reflection White cells (Ballard *et al.* 1994; Newnham and Ballard 1998) in the laboratory, the near-infrared and visible spectra of pure water vapour and water vapour in air were measured at two temperatures (252 and 296 K) with spectral resolution of 0.03 cm^{-1} at the

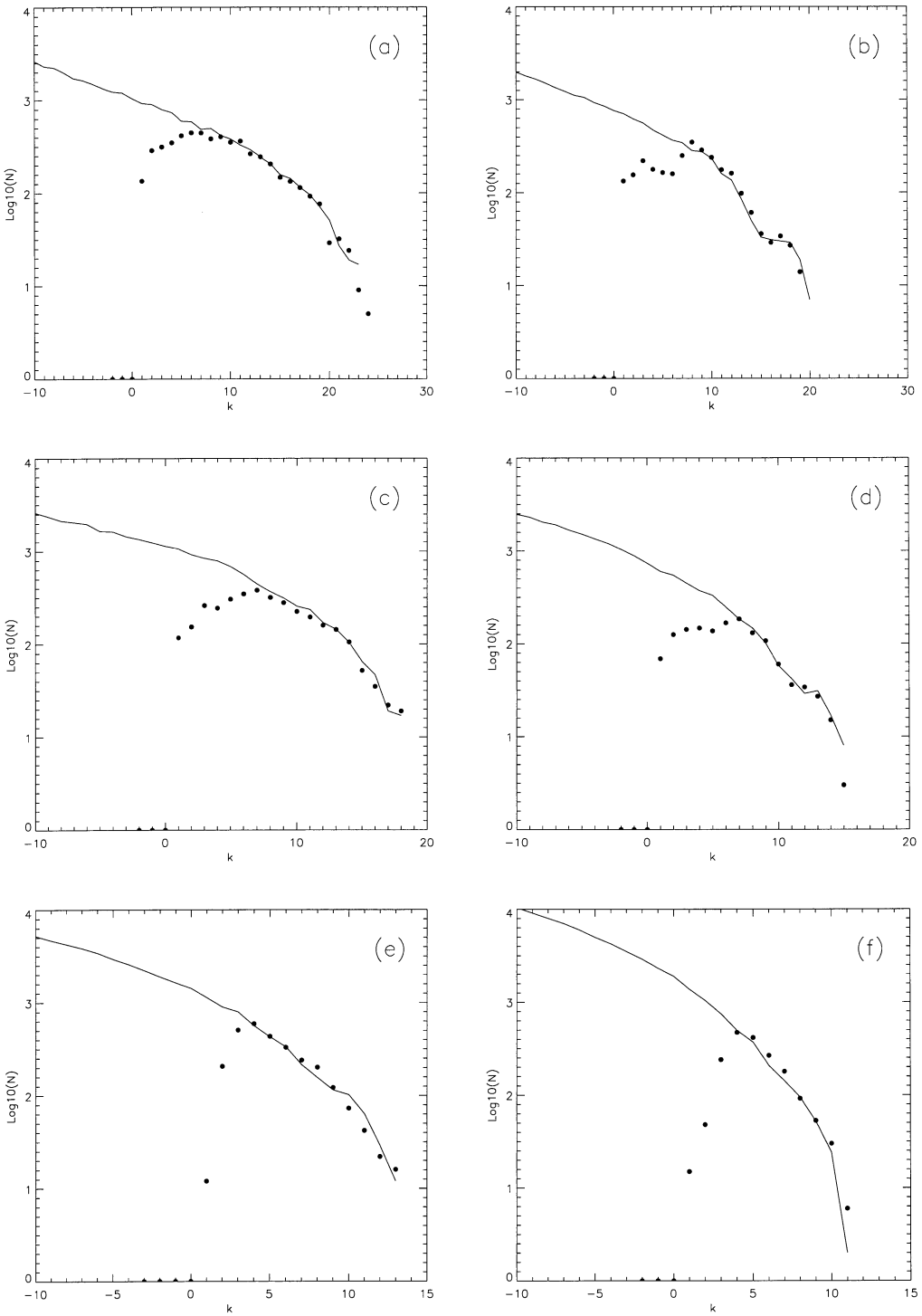

Figure 1. Water vapour line statistics (solid lines) predicted by *ab initio* theory for spectral intervals: (a) 6200 to 8200 cm^{-1}, (b) 8200 to 9700 cm^{-1}, (c) 9700 to 11 500 cm^{-1}, (d) 11 500 to 13 200 cm^{-1}, (e) 13 200 to 16 500 cm^{-1} and (f) 16 500 to 22 700 cm^{-1}. The dots represent the HT96 water vapour line intensity distribution (see text for the definition of N and index k).

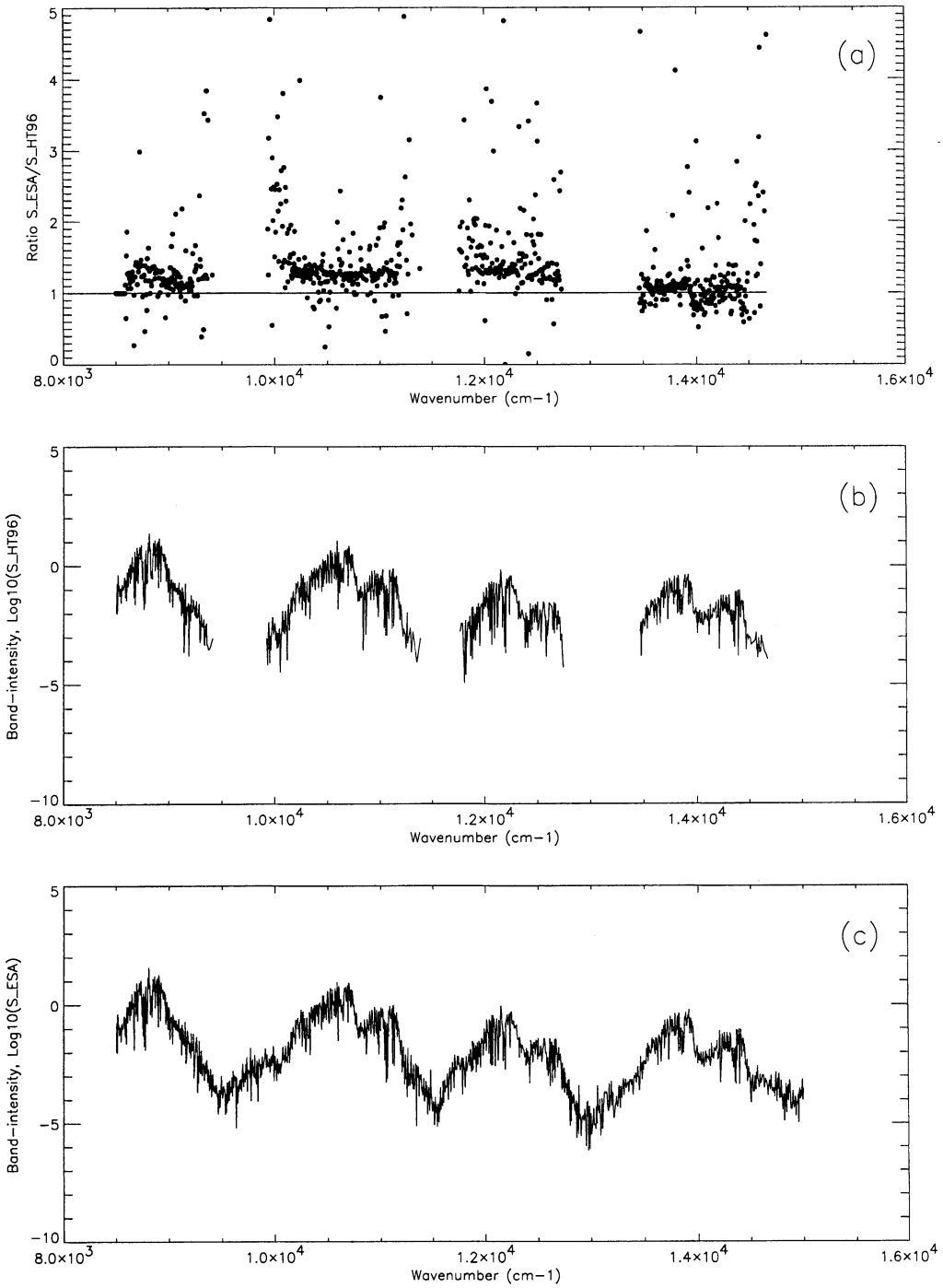

Figure 2. (a) Ratios of random-band-model parameter (band-intensity, in cm^2g^{-1}, for 5 cm^{-1} spectral intervals) derived from the ESA-WVR database to that from HT96. (b) Band-intensity for HT96, and (c) band-intensity for ESA-WVR. See text for details.

TABLE 1. LINE-BY-LINE CALCULATIONS PERFORMED FOR THIS STUDY

Experiment	Spectral region	Database
HT96	1000–22 700 cm^{-1}	HT96 (Rothman *et al.* 1998)
COR	8036–22 700 cm^{-1}	HT96+Corrections (Giver *et al.* 2000)
WEAK	1000–22 700 cm^{-1}	HT96+PS-weak lines (PS 1997)
ESA-WVR	8600–15 000 cm^{-1}	New database (Schermaul *et al.* 2000)

Rutherford Appleton Laboratory. These measurements were taken over a wider range of experimental conditions than those made in the 1980s, and used as the basis of HT96; they included careful analysis of the measurement errors contributing to the accuracy of the final results (see Belmiloud *et al.* 2000). The new data, derived by line-by-line profile fitting and reinforced using sophisticated theoretical calculations, are believed to be an improvement on the current HITRAN listing. The detailed description of the measurements and the new linelist database, called ESA-WVR, can be found in Schermaul *et al.* (2001a,b). The comprehensive database consists of over 36 000 water transitions in the region 8600–15 000 cm^{-1}.

In order to compare the HITRAN and ESA-WVR databases, the narrow-band parameter (sum of line intensities) has been calculated for each database in 5 cm^{-1} spectral intervals using the random-model convention of Rodgers and Walshaw (1966). These are shown in Fig. 2(b) and (c). There are no gaps in the ESA-WVR plot because of the inclusion of the theoretically predicted weak lines. Figure 2(a) shows the ratio of the ESA-WVR to HT96 parameters (where the latter exceeds a certain threshold, taken as 10^{-10} cm^2g^{-1}). It can be seen that the band-intensities of the new linelist are systematically larger than HT96; the ratios range from 0 to 5 but the dominant values are between 1 and 1.5.

3. RADIATIVE TRANSFER MODEL

The GENLN2(v4.0) line-by-line code (Edwards 1992) was modified for the calculation of radiative transfer at solar wavelengths. The solar irradiance at top of atmosphere compiled by Kurucz (1991) is employed, which presents the solar spectrum at a spectral resolution of 1 cm^{-1}, the highest available at present. The solar zenith angle (SZA) is included in the transmission calculation for the downward direct beam, and a five-point Gaussian quadrature is used to calculate the diffuse transmission for the upward diffuse beam. In this work we consider only water vapour absorption; scattering has been neglected.

The line-by-line calculations are performed for three cases used in the Intercomparison of Radiation Codes in Climate Models (ICRCCM, see Ellingson *et al.* 1991): mid-latitude summer (MLS), tropical (TROP) and subarctic winter (SAW), and water vapour is the only absorber considered. Vertical inhomogeneity in the atmosphere is modelled using 60 layers spanning pressure levels from the top of atmosphere to the surface (as in Clough *et al.* 1992). The water vapour continuum is not included. The surface albedo is 0.2; SZAs of 30° and 75° are considered. The Voigt line profile is employed.

For each SZA and for each of the three atmospheric profiles, the line-by-line calculation was carried out with each of the four spectral line databases described in the preceding section. Table 1 summarizes the experiments conducted.

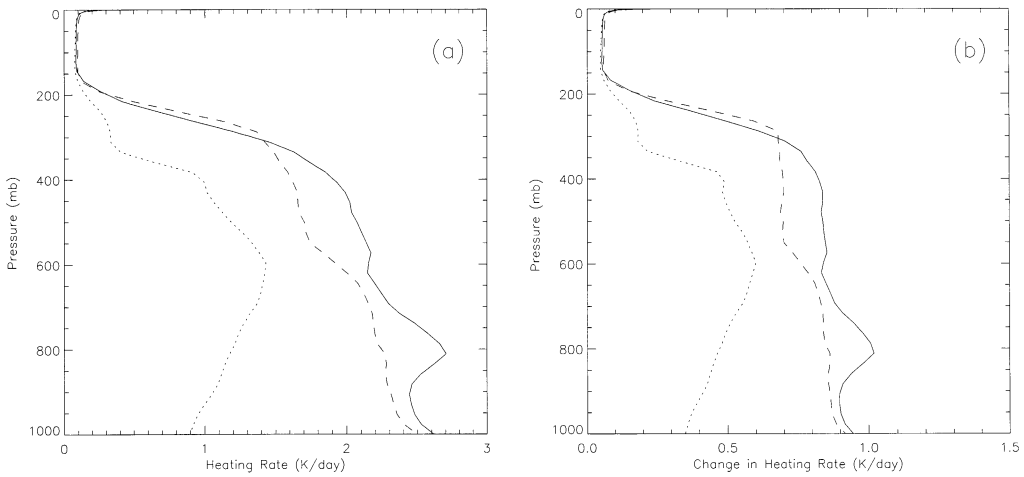

Figure 3. Vertical profiles of the heating rates calculated with a line-by-line model for three atmospheric profiles: TROP (solid line), MLS (dashed line), and SAW (dotted line) due to absorption of solar radiation by water vapour, for solar zenith angles (a) 30° and (b) 75°. See text for details.

4. RESULTS

(*a*) *Heating rates using HT96 spectral data*

Figure 3(a) and (b) shows the vertical distribution of heating rates in the three atmospheres for SZAs of 30° and 75° respectively. Solar heating rates in the troposphere from this study differ from the results of Ramaswamy and Freidenreich (1991; henceforth RF) generally by <4% but by 7–8% for the TROP and MLS atmospheres near the surface. There are relatively larger differences in heating rate (10%) in the SAW middle troposphere. While the use of different incident solar irradiance datasets may be one source of the different results from the two studies, the main cause is believed to be the changes in spectral line parameters from the compilations of the Air Force Geophysics Laboratory (AFGL; Rothman *et al.* 1983) used by RF in HT96.

(*b*) *Downward solar flux*

Figure 4 shows the downward solar spectral irradiance at the surface for the MLS atmosphere for SZA 30° calculated using HT96, as well as the difference in irradiance calculated using COR, WEAK, and ESA-WVR. It can be seen that COR has the smallest effect on solar absorption among the three models, and actually produces reduced absorption in the 8000–9500 and 13 500–17 000 cm^{-1} regions. WEAK has large effects between 5000 and 18 000 cm^{-1}, and ESA-WVR shows strongly increased absorption throughout the region where it exists, 8600–15 000 cm^{-1}.

Table 2 shows the absorption of downward solar radiation within the atmosphere for HT96, integrated over 8600–15 000 cm^{-1} for the three atmospheres and two SZAs, and the differences between WEAK/ESA-WVR and HT96. The numbers in brackets represent the values over the full spectral range available in each case (see Table 1). It can be seen that compared with HT96 results, the absorbed downward solar fluxes of ESA-WVR increase by 5.5, 4.8 and 2.2 W m^{-2} (SZA = 30°) and by 2.4, 2.1 and 1.1 W m^{-2} (SZA = 75°) respectively. This effect is larger than most individual minor absorption bands of other gases. Compared with HT96, WEAK increases absorption by

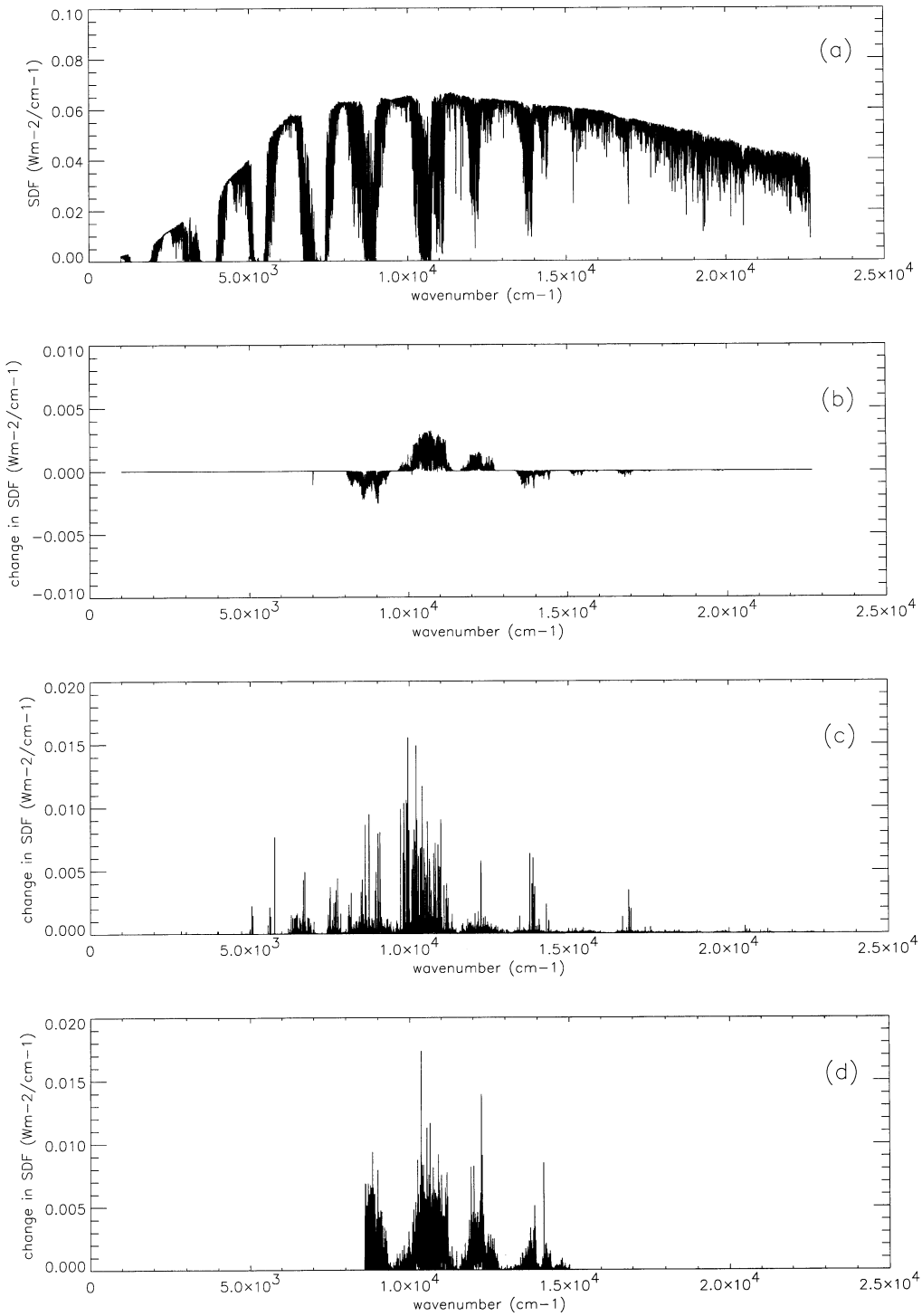

Figure 4. (a) Downward solar flux at the surface (for MLS and solar zenith angle 30°) calculated with HT96 water vapour line data. (b) Difference in downward solar flux between HT96 and COR; (c) as (b) but between HT96 and WEAK; (d) as (b) but between HT96 and ESA-WVR. See text for details.

TABLE 2. ABSORPTION WITHIN THE ATMOSPHERE FOR HT96 (W m^{-2}) AND DIFFERENCES BETWEEN HT96 AND OTHER DATASETS IN THE 8600–15 000 cm^{-1} REGION

SZA:	30°			75°		
Atmosphere:	TROP	MLS	SAW	TROP	MLS	SAW
HT96	70.2	59.9	20.8	32.5	28.8	12.1
	(190.2)	(171.8)	(91.8)	(76.9)	(70.2)	(39.9)
WEAK–HT96	2.0	1.6	0.4	1.1	0.9	0.2
	(2.7)	(2.1)	(0.5)	(1.6)	(1.3)	(0.3)
ESA-WVR–HT96	5.5	4.8	2.2	2.4	2.1	1.1
CONTINUUM:	11.4	9.2	2.4	7.2	5.8	1.7
	(24.1)	(19.5)	(7.4)	(15.5)	(12.4)	(4.0)

Numbers in brackets refer to the full spectral range available.

TABLE 3. ABSORPTION WITHIN THE ATMOSPHERE FOR COR (W m^{-2}) AND DIFFERENCES BETWEEN COR AND OTHER DATASETS IN THE 8600–15 000 cm^{-1} REGION AND ITS FOUR SPECTRAL BANDS (cm^{-1})

SZA:		30°			75°		
Atmosphere:		TROP	MLS	SAW	TROP	MLS	SAW
8 600–15 000	COR	71.37	61.01	21.31	32.91	29.14	12.32
(1 000–22 700)		(191.15)	(172.71)	(92.35)	(77.19)	(70.52)	(40.11)
8 600–9 700	COR	24.56	21.63	8.69	9.96	9.19	4.61
	COR–HT96	−0.50	−0.47	−0.22	−0.14	−0.15	−0.10
	ESA-WVR–COR	1.44	1.42	0.95	0.41	0.40	0.35
9 700–11 500	COR	32.57	28.15	10.08	14.27	12.86	5.77
	COR–HT96	1.58	1.49	0.75	0.49	0.49	0.34
	ESA-WVR–COR	1.44	1.18	0.34	0.71	0.60	0.20
11 500–13 000	COR	6.54	5.20	1.23	3.93	3.22	0.91
	COR–HT96	0.32	0.26	0.08	0.16	0.14	0.05
	ESA-WVR–COR	1.04	0.81	0.20	0.66	0.53	0.13
13 000–15 000	COR	7.70	6.03	1.31	4.75	3.88	1.03
	COR–HT96	−0.23	−0.19	−0.04	−0.13	−0.11	−0.03
	ESA-WVR–COR	0.42	0.36	0.10	0.20	0.17	0.06

2.0, 1.6 and 0.4 W m^{-2} (SZA = 30°) and by 1.1, 0.9 and 0.2 W m^{-2} (SZA = 75°) which is less than ESA-WVR but still significant.

The absorption of downward solar radiation due to the water vapour continuum is also shown in Table 2, which was estimated by taking differences between results from HT96 with and without the continuum model of Clough *et al.* (1989). It can be seen that the effects of ESA-WVR are accounting for approximately from 30 to 90% of the absorption of the water vapour continuum in the 8600–15 000 cm^{-1} spectral region. As the Clough *et al.* model is based on an empirical fit to observations taking into account known spectral lines, our results suggest that the continuum parameters may have to be reduced in this spectral region.

Table 3 shows the absorption of downward solar radiation within the atmosphere for COR, integrated over 8600–15 000 cm^{-1}, and decomposed into the four main water vapour bands, for the same atmospheres as in Table 2. Also shown is the difference between COR and HT96 and between ESA-WVR and COR. The inclusion of the COR corrections into HT96 results in increased absorption of 1.58 W m^{-2} and 0.32 W m^{-2} in the 9700–11 500 and 11 500–13 000 cm^{-1} bands, respectively, but a small reduction in absorption in the other bands. The net effect is a small but non-negligible increase in absorption of 1.17 W m^{-2}. Relative to COR, ESA-WVR increases absorption by 4.3, 3.8

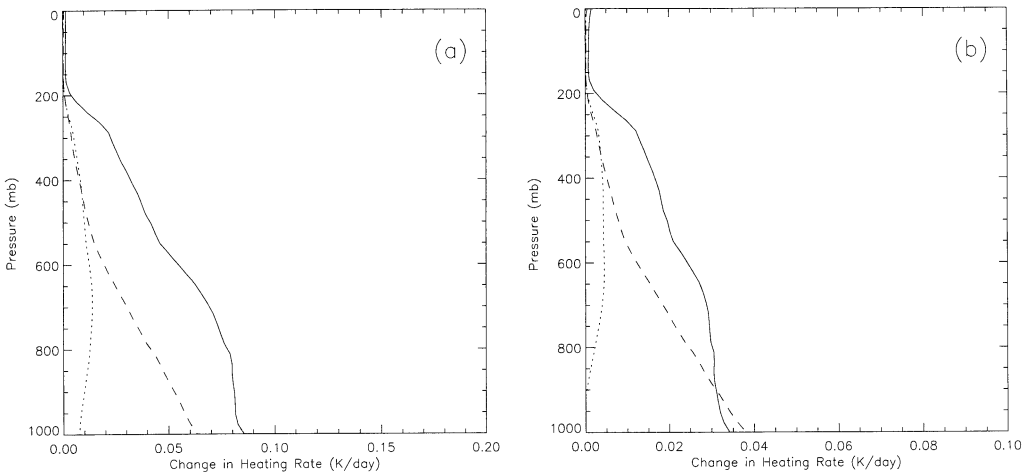

Figure 5. MLS atmospheric vertical profiles of change in heating rate caused by ESA-WVR (solid line), WEAK (dashed) and COR (dotted) for solar zenith angles (a) 30° and (b) 75°. See text for details.

TABLE 4. MAXIMUM HEATING RATES OF HT96 AND MAXIMUM DIFFERENCES IN HEATING RATE (K DAY^{-1}) IN THE 8600–15 000 cm^{-1} REGION

SZA:	30°			75°		
Atmosphere:	TROP	MLS	SAW	TROP	MLS	SAW
HT96	1.47	1.38	0.40	0.57	0.52	0.21
	(2.70)	(2.50)	(1.43)	(1.02)	(0.92)	(0.60)
WEAK–HT96	0.054	0.045	0.009	0.031	0.024	0.005
	(0.079)	(0.064)	(0.010)	(0.049)	(0.038)	(0.006)
(ESA-WVR)–HT96	0.098	0.086	0.036	0.040	0.034	0.016

Numbers in brackets refer to the full spectral range available.

and 1.6 W m^{-2} (SZA = 30°) and by 2.0, 1.7 and 0.8 W m^{-2} (SZA = 75°). These values are slightly less than between HT96 and ESA-WVR. The largest fractional increase in absorption (15.9%) is in the 11 500–13 000 cm^{-1} band, increases in the other bands range from 4.4 to 5.9%.

(*c*) *Heating rates*

Figure 5 presents the vertical profiles of changes in heating rate (K day^{-1}) between COR/WEAK/ESA-WVR and HT96 for the MLS atmosphere. The largest effect is in the lower troposphere for ESA-WVR, near the surface for WEAK and in the middle troposphere for COR. If we consider the full spectral range, WEAK has larger effects than ESA-WVR near the surface for the MLS and TROP atmospheres at the larger solar zenith angle.

Table 4 gives the maximum HT96 heating rates and maximum differences in heating rate between HT96 and WEAK/ESA-WVR for the three atmospheres and two SZAs. Similarly, Table 5 gives the maximum COR heating rates and maximum differences in heating rate between COR and HT96/ESA-WVR. They indicate that the absolute changes in heating rate for the three databases are quite small, mostly less than 0.1 K day^{-1}, but the maximum percentage changes in heating rate are about 7% for ESA-WVR to COR, 5% for WEAK to HT96, and 2% for COR to HT96 in the spectral region 8600–15 000 cm^{-1}.

TABLE 5. AS TABLE 4 BUT FOR COR

SZA:	30°			75°		
Atmosphere:	TROP	MLS	SAW	TROP	MLS	SAW
COR	1.49	1.40	0.41	0.60	0.53	0.22
	(2.71)	(2.52)	(1.44)	(1.06)	(0.95)	(0.64)
COR–HT96	0.018	0.016	0.010	0.006	0.006	0.004
	(0.014)	(0.014)	(0.01)	(0.005)	(0.005)	(0.004)
(ESA-WVR)–COR	0.081	0.073	0.024	0.039	0.033	0.012

5. CONCLUSIONS

In this work we have discussed the impact of new water vapour line parameters, both experimentally determined and theoretically predicted, in the spectral region 8600–15 000 cm^{-1} on atmospheric absorption of solar radiation. The additional absorption due to weak water vapour lines in the region of 1000–22 700 cm^{-1}, predicted by *ab initio* theory, has also been estimated. These are compared with the impact of recent corrections to HT96 by Giver *et al.* (2000). Our calculations show that the corrections to HT96 published by Giver *et al.* (2000) increase absorption and heating by about 1–2%. Even in the corrected database (COR) there is a systematic underestimate of strong line intensities and the omission of numerous weak lines in the 8600–15 000 cm^{-1} spectral region, which cause a reduction in calculated absorbed solar flux of 6–7%, or about 2% of the total absorption in the 8036–22 700 cm^{-1} region, and an underestimate of heating rates by about 5–7%. The omission in HT96/COR of weak water lines alone causes the fluxes to be underestimated by about 0.5–2% and heating rates by about 2–5%. Our calculated additional absorption ranges approximately from 30–90% of the absorption currently ascribed to the water vapour continuum (Clough *et al.* 1989) in the 8600–15 000 cm^{-1} region.

We recommend that the new dataset ESA-WVR should be used in atmospheric radiative transfer models in the 8600–15 000 cm^{-1} region, and that the forthcoming new version of HITRAN database should consider inclusion of these new results. The ESA-WVR dataset can be obtained through ftp from ftp://ftp.tampa.phys.ucl.ac.uk/pub/ESA.

ACKNOWLEDGEMENTS

We would like to acknowledge the invaluable advice and guidance given to us by Dick Learner whose death in December 2000 leaves the field of molecular spectroscopy bereft of a unique talent. We thank Dr Nikolai Zobov for providing weak water line data. This work was supported by the UK Natural Environment Research Council.

REFERENCES

Arking, A. 1996 Absorption of solar energy in the atmosphere: discrepancy between model and observations. *Science*, **273,** 496–499

Ballard, J., Strong, K., Remedios, J. J., Page, M. and Johnston, W. B. 1994 A coolable long path absorption cell for laboratory spectroscopic studies of gases. *J. Quant. Spectrosc. Radiat. Transfer*, **52,** 677–691

Belmiloud, D., Schermaul, R., Smith, K. M., Zobov, N. F., Brault, J. W., Learner, R. C. M., Newnham, D. A. and Tennyson, J. 2000 New studies of the visible and near-infrared absorption by water vapour and some problems with the HITRAN database. *Geophys. Res. Lett.*, **27,** 3703–3706

Cess, R. D., Zhang, M. H., Minnis, P., Corsetti, L., Dutton, E. G., Forgan, B. W., Garber, D. P., Gates, W. L., Hack, J. J., Harrison, E. F., Jing, X., Kiehl, J. T., Long, C. N., Morcrette, J. J., Potter, G. L., Ramanathan, V., Subasilar, B., Whitlock, C. H., Young, D. F. and Zhou, Y. 1995 Absorption of solar-radiation by clouds—observations versus models. *Science*, **267,** 496–499

Chou, M-D. 1999 Atmospheric solar heating in minor absorption bands. *Terr. Atmos. Ocean. Sci.*, **10,** 511–528

Clerbaux, C. 1999 'New water vapour measurements and their impact on the atmospheric radiative budget'. IUGG XXII General Assembly 1999, Birmingham, UK (MC08/E/02-A3)

Clough, S. A., Kneizys, F. X. and Davies, R. W. 1989 Line shape and the water vapor continuum. *Atmos. Res.*, **23,** 229–241

Clough, S. A., Iacono, M. J. and Moncet, J. L. 1992 Line-by-line calculation of atmospheric fluxes and cooling rates: Application to water vapor. *J. Geophys. Res.*, **97,** 15761–15785

Edwards, D. P. 1992 'GENLN2: A general line-by-line atmospheric transmittance and radiance model'. NCAR Technical Note TN367, Boulder, Colorado, USA

Ellingson, R. G., Ellis, J. and Fels, S. 1991 The intercomparison of radiation codes used in climate models: Longwave results. *J. Geophys. Res.*, **96,** 8929–8953

Giver, L. P., Chackerian, C. Jr. and Varanasi, P. 2000 Visible and near-infrared $H_2{}^{16}O$ line intensity corrections for HITRAN-96. *J. Quant. Spectrosc. Radiat. Transfer*, **66,** 101–105

Kurucz, R. L. 1991 The solar spectrum. Pp. 663–669 in *Solar interior and atmosphere*. Eds. A. N. Cox, W. C. Livingston and M. S. Matthews. University of Arizona Press, Tucson, USA

Learner, R. C. M., Zhong, W., Haigh, J. D., Belmiloud, D. and Clarke, J. 1999 The contribution of unknown weak water vapour lines to the absorption of solar radiation. *Geophys. Res. Lett.*, **26,** 3609–3612

Lubin, D., Vogelmann, A., Pamela, J. L., Kressin, A., Ehramjian, J. and Ramanathan, V. 2000 Validation of visible/near-IR atmospheric absorption and solar emission spectroscopic models at 1 cm^{-1} resolution solar radiation. *J. Geophys. Res.*, **105,** 22445–22454

Mlawer, E. J., Brown, P. D., Clough, S. A., Harrison, L, C., Michalsky, J. J., Kiedron, P. W. and Shipport, T. 2000 Comparision of spectral direct and diffuse solar irradiance measurements and calculations for cloud-free conditions. *Geophys. Res. Lett.*, **27,** 2653–2656

Newnham, D. A. and Ballard, J. 1998 Visible absorption cross-sections and integrated absorption intensities of molecular oxygen (O_2 and O_4). *J. Geophys. Res.*, **103,** 28801–28816

Partridge, H. and Schwenke, D. W. 1997 The determination of an accurate isotope dependent potential energy surface for water from extensive *ab initio* calculations and experimental data. *J. Chem. Phys.*, **106,** 4618–4639

Ramaswamy, V. and Freidenreich, S. M. 1991 Solar radiative line-by-line determination of water vapour absorption and water cloud extinction in inhomogeneous atmospheres. *J. Geophys. Res.*, **96,** 9133–9157

Rodgers, C. D. and Walshaw, C. D. 1966 The computation of infrared cooling rate in planetary atmospheres. *Q. J. R. Meteorol. Soc.*, **92,** 67–92

Rothman, L. S., Gamache, R. R., Barbe, A., Goldman, A., Gillis, J. R., Brown, L. R., Toth, R. A., Flaud, J. -M. and Camy-Peyret, C. 1983 AFGL atmospheric absorption line parameter compilations: 1982 edition. *Appl. Opt.*, **22,** 2247–2256

Rothman, L. S., Gamache, R. R., Goldman, A., Brown, L. R., Toth, R. A., Pickett, H. M., Poynter, R. L., Flaud, J. -M., Camy-Peyret, C., Barbe, A., Husson, H., Rinsland, C. P. and Smith, M. A. H. 1987 The HITRAN database: 1986 edition. *Appl. Opt.*, **26(19),** 4058–4097

Rothman, L. S., Gamache, R. R., Tipping, R. H., Rinsland, C. P., Smith, M. A. H., Benner, D. C., Devi, V. M., Flaud, J. -M., Camy-Peyret, C., Perrin, A., Goldman, A., Massie, S. T., Brown L. R. and Toth, R. A. 1992 The HITRAN molecular database: Editions of 1991 and 1992. *J. Quant. Spectrosc. Radiat. Transfer*, **48,** 469–507

Rothman, L. S., Rinsland, C. P., Goldman, A., Massie, S. T., Edwards, D. P., Flaud, J. -M., Perrin, A., Camy-Peyret, C., Dana, V., Mandin, J. Y., Schroeder, J., McCann, A., Gamache, R. R., Wattson, R. B., Yoshino, K., Chance, K. V., Jucks, K. W., Brown, L. R., Nemtchinov, V. and Varanasi, P. 1998 The HITRAN molecular spectroscopic database and HAWKS (HITRAN Atmospheric Workstation): 1996 edition. *J. Quant. Spectrosc. Radiat. Transfer*, **60,** 665–710

Schermaul, R., Learner, R. C. M., Newnham, D. A., Williams, G. R., Ballard, J., Zobov, N. F., Belmiloud, D. and Tennyson, J. 2001a The water vapour spectrum in the region 8600–15000 cm^{-1}: experimental and theoretical studies for a new spectral line database I: Laboratory measurements. *J. Mol. Spectrosc.*, in press

Schermaul, R.,Learner, R. C. M., Newnham, D. A., Ballard, J., Zobov, N. F., Belmiloud, D. and Tennyson, J. 2001b The water vapour spectrum in the region 8600–15000 cm^{-1}: experimental and theoretical studies for a new spectral line database II: Linelist construction. *J. Mol. Spectrosc.*, in press